Sensitivity of catalysis to surface structure: The example of CO oxidation on Rh under realistic conditions

J. Gustafson,[1,*] R. Westerström,[2] A. Mikkelsen,[2] X. Torrelles,[3] O. Balmes,[4] N. Bovet,[5] J. N. Andersen,[2] C. J. Baddeley,[1] and E. Lundgren[2]

[1]*EaStCHEM School of Chemistry, University of St Andrews, St Andrews, Fife KY16 9ST, United Kingdom*

[2]*Department of Synchrotron Radiation Research, Lund University, Box 118, SE-221 00 Lund, Sweden*

[3]*Instituto de Ciencia de Materiales de Barcelona (CSIC), 08193 Bellaterra, Barcelona, Spain*

[4]*ESRF, 6 rue Jules Horowitz, F-38043 Grenoble Cedex, France*

[5]*MAX-lab, Lund University, Box 118, SE-221 00 Lund, Sweden*

(Received 17 March 2008; published 22 July 2008)

Using a combination of surface x-ray diffraction and mass spectrometry at realistic pressures, the CO oxidation reactivity of Rh(111) and Rh(100) model catalysts has been studied in conjunction with the surface structure. The measurements show that the presence of a specific thin surface oxide is crucial for the high activity of the Rh based CO oxidation. As this oxide is readily formed on all Rh facets, we conclude that the specific Rh crystal planes exposed during catalysis will not directly influence the reactivity. This is fortified by the very close similarity between the Rh(111) and the Rh(100) results.

DOI: 10.1103/PhysRevB.78.045423 PACS number(s): 82.65.+r, 61.05.cp, 68.47.Gh, 82.80.Ms

I. INTRODUCTION

Transition-metal based catalysts, consisting of dispersed active metal nanoparticles on an insulating oxide support, form the basis of much of modern chemistry. These nanoparticles, or nanocrystals, expose various facets, the most abundant of which, in the case of an fcc metal, are the (111) and (100) surfaces due to their low surface energies, according to the Wulff construction.[1] The catalysis related properties of different facets have therefore been extensively explored under ultrahigh vacuum (UHV) conditions, using model single-crystal surfaces, demonstrating that for many reactions, the surface orientations present on the nanoparticle have a strong impact on the catalytic activity.[2–6] At more realistic pressures, the effects of the surface orientation on the catalytic properties is in principle unexplored, both experimentally and theoretically.

A very recent *in situ* reflectance absorption infrared spectroscopy (RAIRS) study of CO oxidation on Pt-group metals under relevant conditions shows the existence of a "hyperactive" oxygen-covered phase.[7] This could agree well with earlier studies showing that the CO oxidation reaction over Pt and Pd model catalysts is more efficient when a thin oxide is present on the substrate surface,[8–10] a situation which may correspond to that of a real catalyst at work. Although such thin oxides have been shown to exist on a number of transition-metal surfaces,[11] their role in catalysis at realistic conditions is under debate.[12]

In the case of Rh, one of the active components in automotive catalytic converters,[13,14] no such studies have been performed previously. It has, however, been shown that in high oxygen partial pressures, a similar thin trilayer O-Rh-O surface oxide is formed on all Rh surface orientations investigated so far.[15–19] These studies include low-index surfaces as well as the (553) and (223) high-index surfaces, where the stepped surface structure completely vanishes during the surface oxide formation.[18,19] A very recent density-functional-theory study by Mittendorfer *et al.*[20] showed that this also applies to Rh nanoparticles.

In the present paper, we have used surface x-ray diffraction (SXRD) and mass spectrometry to investigate the relation between the presence of oxide structures and changes in the CO oxidation activity over Rh(111) and Rh(100) surfaces *in situ* at catalytically relevant pressures. Although there are some minor differences, the general behavior is practically identical for the two surface orientations. Starting with the surface oxide in pure O_2, introducing CO reduces the oxide and leaves the surface in a metallic phase. At this point, mass spectrometry reveals a low CO_2 production. As the reaction proceeds, the O_2/CO ratio in the chamber rises and at one point the surface oxide is reformed. Concurrently, a large increase in the CO oxidation rate can be observed.

The results show that for CO oxidation, the Rh surface is much more active in the surface oxide phase than in the metallic phase. Since a similar surface oxide is formed on all Rh surfaces, including nanoparticles, our results strongly suggest that the reactivity of a Rh based CO oxidation catalyst is not sensitive to the specific crystal planes exposed but is governed by the surface oxide formation. This conclusion is fortified by a very close similarity between the Rh(111) and the Rh(100) results.

II. EXPERIMENT

The measurements were performed in the high-pressure chamber[21] at the surface diffraction beamline ID3 (Ref. 22) at the European Synchrotron Radiation Facility (ESRF) in Grenoble, France. The wavelength of the incident x rays was set to 0.724 Å. The sample was aligned according to the bulk Bragg reflections of the Rh substrates. The coordinates (H,K,L) in reciprocal space refer to a basis $(\mathbf{b}_1,\mathbf{b}_2,\mathbf{b}_3)$ with $\mathbf{b}_1$ and $\mathbf{b}_2$ spanning the surface lattice of the Rh substrate, as shown in Figs. 1(b) and 1(c) for (111) and (100), respectively, and with $\mathbf{b}_3$ perpendicular to the surface plane.

The CO oxidation measurements were performed in a so-called batch reaction chamber, in which the system is first stabilized in the presence of pure O_2. CO is then introduced

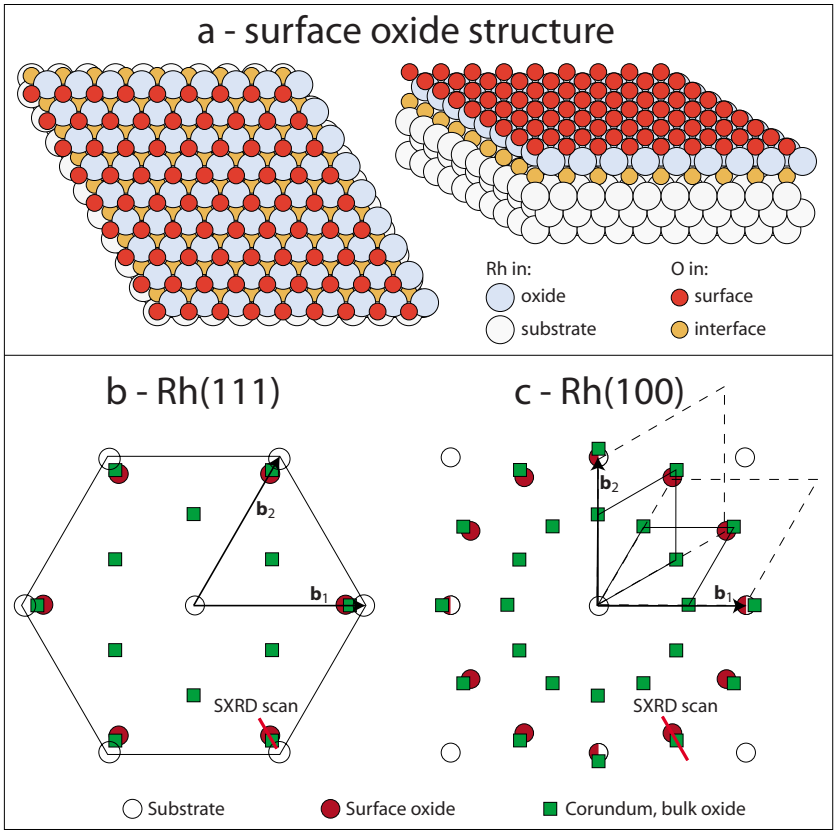

FIG. 1. (Color online) (a) Model of the surface oxide found on all investigated Rh surface orientations, here shown on top of a (111) surface. Maps of the reciprocal spaces corresponding to (b) Rh(111) and (c) Rh(100), including the surface oxide as well as the corundum structured bulk oxide. $\mathbf{b}_1$ and $\mathbf{b}_2$ define the basis in which reciprocal vectors are expressed. The Rh(100) surface shows two domains of each oxide structure, indicated by the dashed (surface oxide) and solid (bulk oxide) unit cells. The red lines show the SXRD scans shown in Figs. 2(c) and 3(c).

into the chamber and the oxidation reaction starts. As one O_2 molecule can oxidize two CO molecules, the O_2/CO pressure ratio is automatically increased as the reaction proceeds, creating a more oxidizing environment. In this way, the partial gas pressures, the surface phase, and the sample temperature can be followed with time during the reaction. At the end of the experiment, we can retrieve the starting conditions by evacuating the gas from the chamber and refilling it with O_2. The CO gas line is specially equipped with a piece of curled copper tubing, which can be heated to 575 K and acts as a trap for Ni carbonyls. The line also has two liquid N_2 traps to further clean the CO by subsequent steps of condensation and distillation.[23]

The crystals were cleaned as in Ref. 16. The sample temperature was measured using a tungsten-rhenium thermocouple (type *C*), mechanically clamped between the ceramic heating plate and the sample clips. Also here Ni was avoided in order to eliminate the risk of Ni carbonyl contamination.

III. RESULTS AND DISCUSSION

Figure 1(a) shows a model of the surface oxide found on all investigated Rh surfaces, built up by three close-packed hexagonal layers of O-Rh-O.[15] Depending on the substrate, the in-plane lattice constant varies between 3.0 and 3.1 Å, which yields coincidence lattices of (9×9) and $c(8\times2)$ with (111) and (100) substrates, respectively. Figures 1(b) and 1(c) show the corresponding reciprocal lattices as seen by SXRD on the (111) and (100) substrates, respectively. In the (100) case, we find two different domain orientations due to the hexagonal structure of the surface oxide and the square substrate. The figure also indicates where the corundum structured bulk Rh oxide would appear if present.

Figure 2 shows the results of a typical experiment on Rh(111). Panel (a) shows the partial pressures of O_2, CO, and CO_2. At $t=-1000$ s, 300 mbar of O_2 and close to no CO and CO_2 are present in the batch reactor. At this time, the diffraction measurements detect the presence of the surface oxide on the surface [Fig. 2(c)]. At time $t=0$, 330 mbar CO is added, and the CO_2 production starts. This is seen in the figure as a slow rise in the CO_2 signal and drop in the O_2 and CO signals. Here, no surface oxide can be detected [Fig. 2(c)]. Since a single O_2 molecule can oxidize two CO molecules into CO_2, the rate of decrease in the CO partial pressure as well as the rate of increase of CO_2 is twice the rate of decrease of O_2. This also ensures that an oxidizing environment is being approached. The spike in the O_2 signal at $t=0$ is due to the CO being added in one side of the chamber, pushing the gas already in the chamber toward the other side where the mass spectrometer is located. At $t\approx3300$ s, we

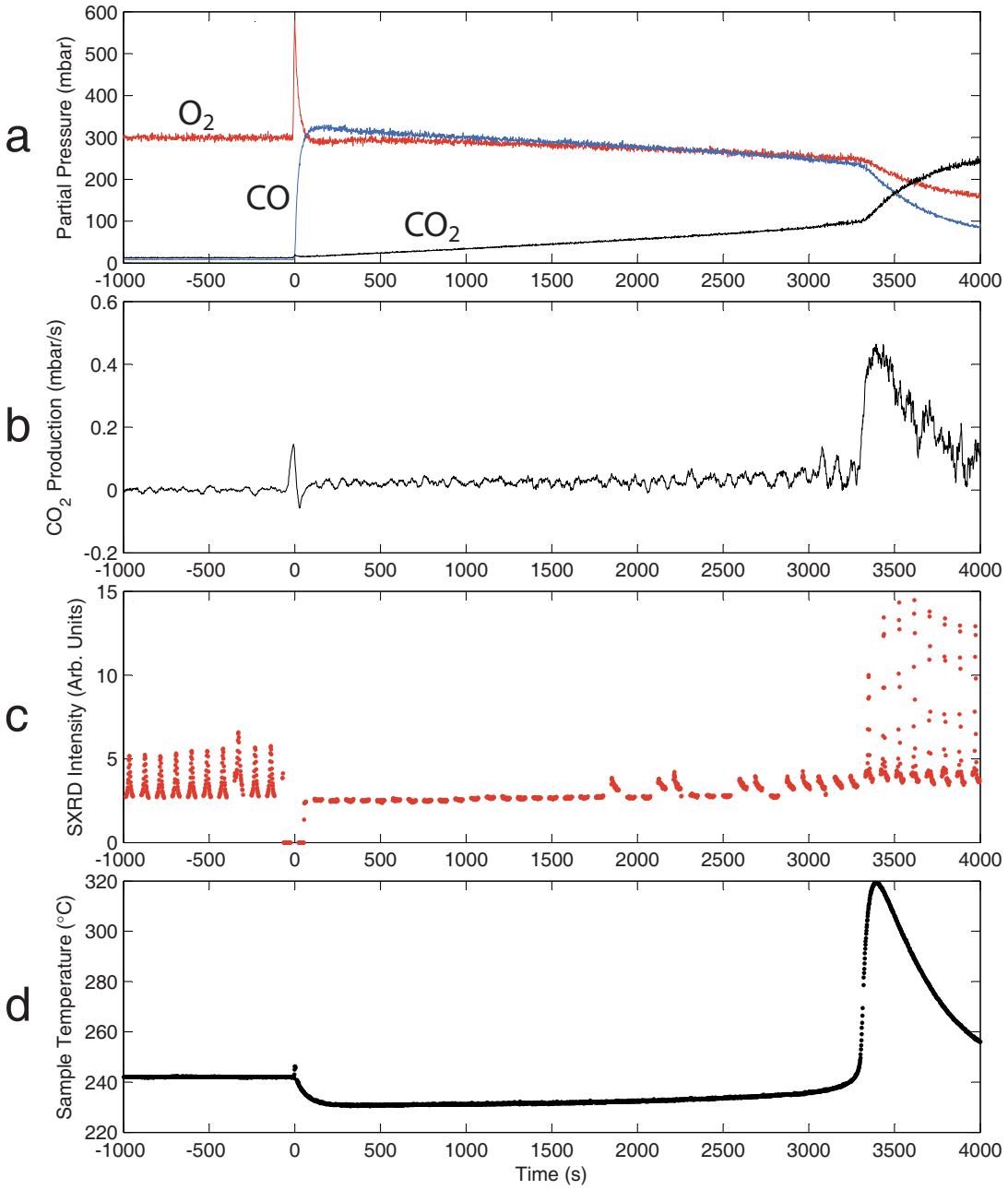

FIG. 2. (Color online) The CO oxidation and surface structure of the Rh(111) surface during realistic reaction conditions. (a) Partial pressures of O_2, CO, and CO_2. The experiments starts in pure O_2, and CO is added at $t=0$, which starts the CO oxidation reaction. As the reaction proceeds, the O_2 and CO pressures decrease, while the CO_2 signal is rising. At $t\approx 3300$ s, there is a sudden increase in the reaction speed, as is directly monitored in (b). (b) The CO_2 production as derived from (a). (c) Consecutive SXRD scans along the red line in Fig. 1(c), showing the presence or absence of the surface oxide. The surface oxide is removed immediately after adding the CO at $t=0$ and reappears simultaneously with the dramatic increase in the reaction rate at $t\approx 3300$ s. (d) Sample temperature during the experiment. Note the dramatic increase in sample temperature simultaneous with the switch to high activity.

notice a significant increase in the reaction rate. This change coincides with the return of the surface oxide as shown in Fig. 2(c). By the end of the experiment, almost all of the CO has been converted into CO_2.

Figure 2(b) shows the CO_2 production rate, i.e., the activity of the model catalyst. From the start there is no CO present and hence no activity. At $t=0$ we find a peak in activity as the surface oxide is reduced, followed by a low but slowly rising reaction rate. At $t\approx 3300$ s, as above, we see a sudden increase in activity as the surface oxide appears.

Figure 2(c) shows consecutive SXRD scans along the line indicated in Fig. 1(b), showing the presence or absence of the surface oxide. As seen in Fig. 1(a), the bulk oxide would also be visible in these scans, but it does not appear throughout the experiment. After adding O_2 at $t=-1000$ s, the surface oxide peak can be detected. The surface oxide is removed immediately when CO is introduced at $t=0$ and reappears again at $t\approx 3300$ s.

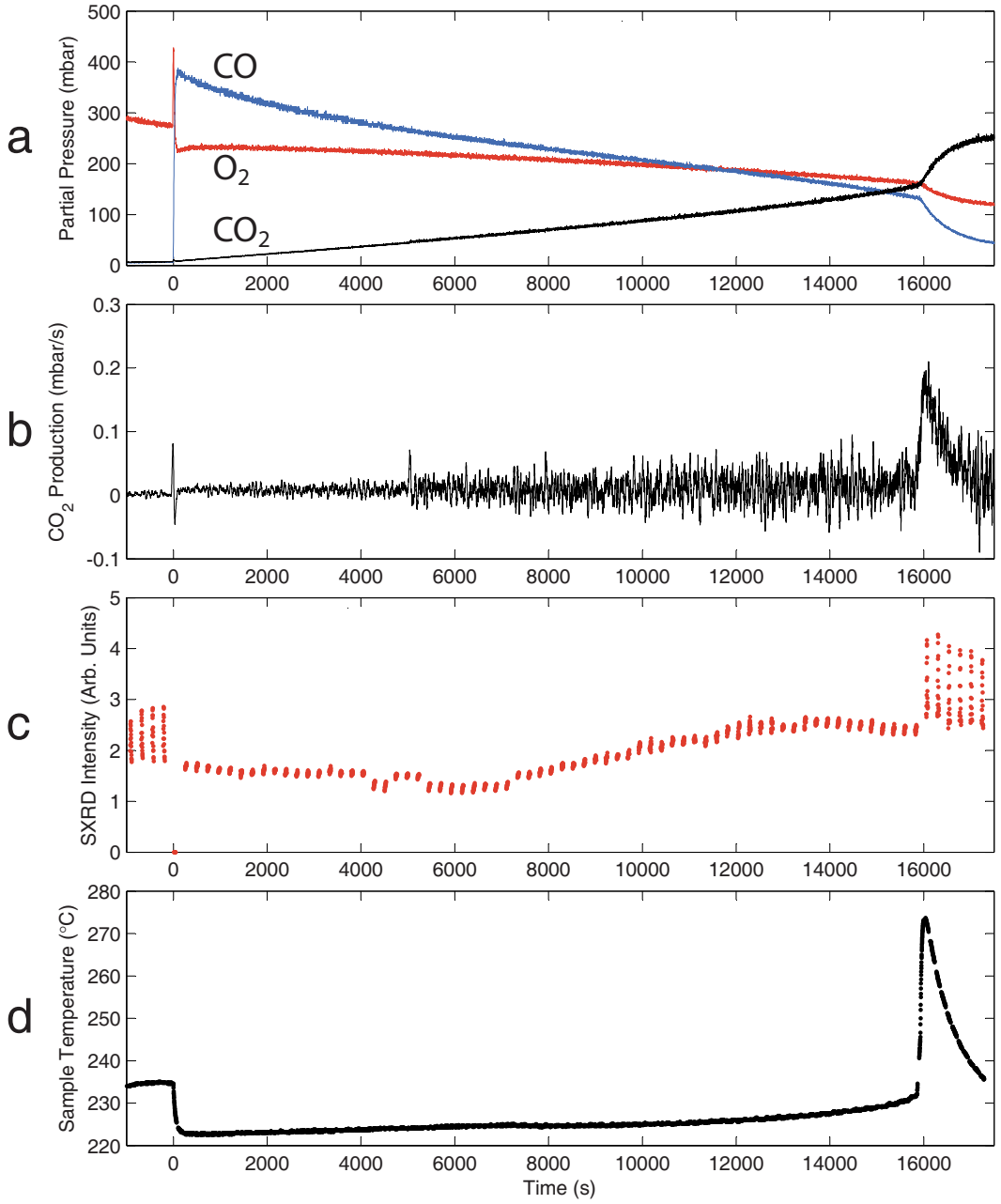

FIG. 3. (Color online) The CO oxidation and surface structure of the Rh(100) surface during realistic reaction conditions. (a) Partial pressures of O_2, CO, and CO_2; (b) CO_2 production; (c) consecutive SXRD scans showing the presence or absence of the surface oxide; and (d) sample temperature during a CO oxidation experiment on Rh(100). For details see Fig. 2.

Shown in Fig. 2(d) is the variation in sample temperature during the experiment. Starting at the preset temperature of about 240 °C, we find a small peak at $t=0$ as the CO is introduced and the surface oxide is reduced. After this, the temperature drops to about 230 °C due to the higher cooling effect of the increased amount of gas in the chamber. In the metallic phase, between $t=0$ and 3300 s, the temperature is slowly rising, and before the switch to the oxidized phase, the temperature is back to about 240 °C. As the oxide returns, the temperature suddenly rises by about 80 °C, due to the exothermic nature of the reaction. The increase in temperature corresponds to an annealing of the sample, which increases the domain size of the surface oxide, explaining the higher and sharper peaks found in Fig. 2(c) at $t>3300$ s as compared to those at $t<0$.

Shown in Fig. 3 is a similar experiment as that above but for the Rh(100) surface. Although there are some apparent differences between the two surfaces, the result is essentially identical to the (111) case.

In summary, the (100) surface is oxidized in 300 mbar O_2 at a temperature of $T\approx 240$ °C, resulting in a surface oxide. No bulk oxide can be detected, either by in-plane scans or by out-of-plane scans under these conditions. At $t=0$ s, 390 mbar CO is introduced into the chamber, which reduces the oxide, leaving the surface in a metallic phase with CO and O competing for the adsorption sites. In this phase we again

find a slow CO oxidation rate, resulting in a rising O_2/CO partial pressure ratio. When the ratio is high enough at $t = 16\,000$ s, the surface oxide is reformed, which coincides with a major rise in the CO_2 production rate.

The longer waiting time between reduction and reoxidation in the Rh(100) case is due to accidentally adding much more CO and simultaneously pumping some O_2 at $t=0$. The lower peak in reaction rate is due to the lower amount of CO available once the surface switches back to the surface oxide phase.

In experiments not shown here, we have found that the Rh bulk oxide is not active in the CO oxidation process. Thus the presence of the surface oxide has to be responsible for the high activity. We cannot, however, rule out that patches of metallic surface coexist with the surface oxide.

As stated above, it has recently been shown that similar surface oxide structures, exhibiting three close-packed layers of O-Rh-O, are found on all investigated surface orientations of Rh, including the low-index (111), (100), and (110) as well as the stepped (553) and (223) orientations.[15–19] In the latter cases, the steps were bunched together, forming large {111} facets containing flat films of the surface oxide. In fact, a $Pt_{25}Rh_{75}(100)$ alloy also behaves in a similar way, as shown in recent experiments.[24] Even Rh nanoparticles has been shown to exhibit a thin oxide film.[25,26] A very recent density-functional-theory (DFT) study by Mittendorfer *et al.*[20] showed that, as in the case of stepped surfaces, the nanoparticles expose surface oxide–covered low-index facets at high oxygen pressures. In combination with the present results, showing that the surface oxide is crucial for the high CO oxidation activity of Rh based catalysts, this strongly suggests that the catalytic activity is not controlled by the detailed structure of the Rh substrate surface itself but rather by the oxidation properties. This, in turn, also means that the surface orientation of the facets plays a minor role in the control of the reactivity, which is strongly supported by the fact that we do not observe any significant differences between the behaviors of the (111) and (100) surfaces.

The difference in reactivity between the (surface) oxidized and metallic Rh surfaces is striking and definitely rules out the metallic surface as solely responsible for the high activity of Rh based CO oxidation catalysts. The exact reaction process cannot be determined from the present measurements. Although UHV based experiments show that CO cannot adsorb on the surface oxide even at 90 K,[27] the increase in chemical potential at higher pressures may still yield reasonable adsorption energies and reaction barriers.[28] On the other hand, recent DFT calculations by Westerström *et al.*[24] showed that CO oxidation on the edge of the Rh surface oxide on $Pt_{25}Rh_{75}(100)$ exhibits significantly lower reaction barriers than on the metallic surface, or on the surface oxide. Thus, the coexistence of the surface oxide and metallic surface areas could be responsible for the highest activity. An alternative explanation could be the presence of defects such as missing O atoms at the surface of the oxide film. Such defects would create undercoordinated Rh sites, suitable for CO adsorption and oxidation, similar to the reaction process in the RuO_2 system.[29] In essence, such a process would be similar to a process at the edge of a surface oxide island as described above.

Our results also agree well with recent *in situ* RAIRS results by Chen *et al.*,[7] showing that a hyperactive oxygen-covered phase can be found at high O_2/CO pressure ratios. In contrast to our findings, however, they reported that the active surface is not oxidized but covered by a monolayer of chemisorbed oxygen. This statement is based on *ex situ* XPS measurements, performed after quenching the active structure by cooling and evacuating the chamber. It is difficult to know whether the structure really stays unchanged through this process. This could explain the different results from the two studies. Another explanation would be that the phase with chemisorbed oxygen is present only in a rather narrow pressure range or slightly different conditions, such that our measurements miss it.

IV. CONCLUSIONS

To conclude, we have studied the relationship between surface structure and CO oxidation reactivity over Rh(111) and Rh(100). Both systems show practically identical behaviors. Starting with the surface covered by a surface oxide, introducing CO reduces this oxide and leaves the system in a metallic low-activity phase. When the O_2/CO pressure ratio is high enough, the surface oxide returns. Concurrently the CO_2 production rate increases dramatically and the sample temperature increases by up to 80 °C. This clearly shows that the surface oxide plays a crucial part in the high activity of a Rh model catalyst. Since the surface oxide is formed on all surface orientations, this strongly indicates that the CO oxidation reactivity on Rh based catalysts is not sensitive to the specific crystal planes exposed during catalysis but is governed by the surface oxide formation. This agrees well with the practically identical behaviors found for Rh(111) and Rh(100).

ACKNOWLEDGMENTS

This work was financially supported by the Swedish Research Council, the Crafoord Foundation, and the Knut and Alice Wallenberg Foundation. Support by the ESRF staff is gratefully acknowledged. The University of St Andrews is a charity registered in Scotland (No. SC013532). X.T. thanks the Spanish M.E.C. Agency for partial funding support through Project No. MAT2005-01736.

*johan.gustafson@st-andrews.ac.uk

[1] G. Wulff, Z. Kristallogr. **34**, 445 (1901).
[2] G. A. Somorjai, *Introduction to Surface Chemistry and Catalysis* (Wiley, New York, 1994).
[3] *Handbook of Heterogeneous Catalysis*, edited by G. Ertl, H. Knözinger, F. Schüth, and J. Weitkamp (Wiley, Weinheim, 2008).
[4] F. Zaera, Prog. Surf. Sci. **69**, 1 (2001).
[5] B. K. Hodnett, *Heterogeneous Catalytic Oxidation* (Wiley, Chichester, UK, 2000).
[6] J. K. Norskov *et al.*, J. Catal. **209**, 275 (2002).
[7] M. S. Chen, Y. Cai, Z. Yan, K. K. Gath, S. Axnanda, and D. W. Goodman, Surf. Sci. **601**, 5326 (2007).
[8] B. L. M. Hendriksen and J. W. M. Frenken, Phys. Rev. Lett. **89**, 046101 (2002).
[9] B. L. M. Hendriksen, S. C. Bobaru, and J. W. M. Frenken, Surf. Sci. **552**, 229 (2004).
[10] M. D. Ackermann *et al.*, Phys. Rev. Lett. **95**, 255505 (2005).
[11] E. Lundgren, A. Mikkelsen, J. N. Andersen, G. Kresse, M. Schmid, and P. Varga, J. Phys.: Condens. Matter **18**, R481 (2006).
[12] G. Rupprechter and C. Weilach, Nanotoday **2**, 20 (2007).
[13] K. C. Taylor, in *Catalysis-Science and Technology*, edited by J. R. Anderson and M. Boudart (Springer-Verlag, Berlin, 1984), Vol. 5, pp. 120–170.
[14] M. Shelef and G. W. Graham, Catal. Rev. - Sci. Eng. **36**, 433 (1994).
[15] J. Gustafson *et al.*, Phys. Rev. Lett. **92**, 126102 (2004).
[16] J. Gustafson *et al.*, Phys. Rev. B **71**, 115442 (2005).
[17] C. Dri, C. Africh, F. Esch, G. Comelli, O. Dubay, L. Köhler, F. Mittendorfer, G. Kresse, P. Dudin, and M. Kiskinova, J. Chem. Phys. **125**, 094701 (2006).
[18] J. Gustafson *et al.*, Phys. Rev. B **74**, 035401 (2006).
[19] J. Klikovits, Ph.D. thesis, Institut für Allgemeine Physik, Technische Universität Wien, 2008.
[20] F. Mittendorfer, N. Seriani, O. Dubay, and G. Kresse, Phys. Rev. B **76**, 233413 (2007).
[21] P. Bernard, K. Peters, J. Alvarez, and S. Ferrer, Rev. Sci. Instrum. **70**, 1478 (1999).
[22] S. Ferrer and F. Comin, Rev. Sci. Instrum. **66**, 1674 (1995).
[23] M. D. Ackermann, Ph.D. thesis, Kamerlingh Onnes Laboratory, Leiden University, 2007.
[24] R. Westerström *et al.*, J. Phys.: Condens. Matter **20**, 184018 (2008).
[25] G. Rupprechter, K. Hayek, and H. Hofmeister, J. Catal. **173**, 409 (1998).
[26] M. A. Newton, A. J. Dent, S. Diaz-Moreno, S. G. Fiddy, B. Jyoti, and J. Evans, Chem.-Eur. J. **12**, 1975 (2006).
[27] E. Lundgren *et al.*, J. Electron Spectrosc. Relat. Phenom. **144-147**, 367 (2005).
[28] J. Rogal, K. Reuter, and M. Scheffler, Phys. Rev. Lett. **98**, 046101 (2007).
[29] H. Over, Y. D. Kim, A. P. Seitsonen, S. Wendt, E. Lundgren, M. Schmid, P. Varga, A. Morgante, and G. Ertl, Science **287**, 1474 (2000).